Review Article

Journal of Ophthalmology & Clinical Research

Progress of the 30-year Laser Vision Technology

Jui-Teng Lin*

New Vision, Inc. Taipei, Taiwan 103

***Corresponding author**
Jui-Teng Lin, New Vision, Inc. Taipei, Taiwan 103, E-mail: jtlin55@gmail.com.

Submitted: 18 Dec 2016; **Accepted:** 08 Jan 2017; **Published:** 12 Jan 2017

Abstract

This review paper will consist of: (1) A historical review of the 30 years progress of laser vision corrections (1987 to 2016); (2) Summary of eye lasers and their applications; (3) Recent developments and new trends; (4) The principles and formulas of laser and non-laser vision corrections; and (5) UV-light-initiated corneal collagen crosslinking.

Keywords: Lasers, Vision correction, Corneal cross linking, Refractive surgery.

Historical Review

The first human trial of PRK was conducted by Dr. Trokel in 1987, based upon the IBM patent (UV laser for organic tissue ablation) and the animal study in 1983. FDA approval PRK in 1995. The flying-spot scanning technology was invented by Dr. J.T. Lin in 1992 (US patent) who also introduced the customized procedure in 1996. The waveguide device was commercialized in 1999. FDA approved LASIK in 2002. During 1995-1999, various laser systems/procedures were developed including: LTK (using Ho:YAG), DTK (using diode laser), RF and CK designed for hyperopia corrections; slide state lasers (YAG-213 nm for PRK), YAG pico-second-PRK, Mini-Excimer for PRK etc. Technologies developed in the 2000's include: eye-tracking device (Lai, Nvatek), microkeratome, Elevation map, topography-guided LASIK, wavefront for customized LASIK (Tracey), presbyopia treatment using SEB (Schachar) and laser scleral-ablation for presbyopia (Lin); accommodative IOL.

More recently, femto-second lasers are developed for flat cutting, stroma ablation and cataract. UV-light and riboflavin activated corneal cross linking (CXL) has been developed for clinical use for various corneal deceases such as corneal keratoconus, corneal keratitis, corneal ectasia, corneal ulcers, and thin corneas prior to LASIK vision corrections. Combined technology of CXL-PRK, CXL-intra stroma-femto-laser pocket, CXL-phakic-IOL, CXL-IC-ring.

Eye lasers and applications [1-4]

As shown in Table 1, various eye lasers have been developed for both vision and non-vision treatments. Figure 1 shows vision technology using various lasers action on the corneal surface, scleral, crystal lens or retinal for various applications. As shown in Figures 2 and 3, LASIK system using a flying spot scanning method and the solid state UV-213 nm system (patented by Lin, 1992).

Recent developments and new trends

New laser technology trends shall include: high-power and pulsed cross linking (CXL) and its new applications; endo-assisted glaucoma and non-invasive-presbyopia lasers; femto-laser new applications (for cataracts, lens surface ablation), new solid-state UV-laser for LASIK, and multi-wavelength systems for multi-applications (such as 3- wavelength, green, blue and yellow lasers for retina, AMD treatments).

Laser (wavelength, pulse width)	Applications
Excimer ArF (193 nm, 5-20 n.s.)	PRK, LASIK, LASEK
Excimer XeCl (308 nm, 200 n.s.)	Glaucoma
Argon Ion (488/514 nm, CW)	Coagulation, glaucoma
Diode laser (810 nm, cw) (1.4 to 2.1 micron, cw)	TTT (CNV, AMD glaucoma/ TCPC DTK (hyperopia)
(5) Nd:YAG (1064 nm, pulsed)	posterior capsulotomy, phaco
(6) Green Nd:YAG (532 nm, 3-10 n.s.) Yellow Nd:YAG (580 nm, cw) Blue Nd:YAG (460 nm, cw)	PDT (for CNV or AMD)
UV:YAG (213-266 nm, 3-20 n.s.)	LASIK, LAPR (presbyopia)
Ho:YAG (2.1 micron, 200 us)	LTK (hyperopia)
Er:YAG and YSGG (2.8-2.94 micron, 200 u.s)	LAPR (presbyopia), phaco emulsi-fication, blepharoplasty
CO_2 (10.6 micron, ultra-pulsed)	Blepharoplasty
Femto-laser (1047 nm, ultarshort pulse)	femto-flat, femto-pocket, fem-to-lens
UV diode laser or LED (365 nm)	corneal cross linking (CXL)

Table 1: Summary of Ophthalmic Lasers and Applications.

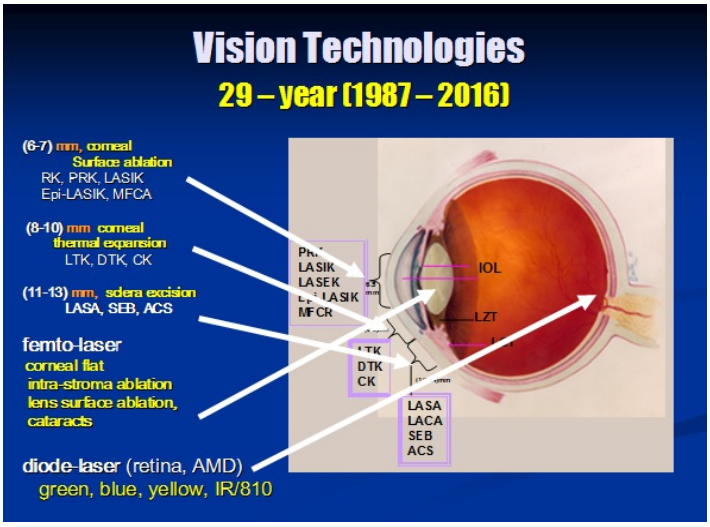

Figure 1: Various laser technologies acting on the corneal surface (6-8 mm), scleral (8-13 mm), intrastroma, crystal lens, and retina for PRK, LASIK, LAPR, ACS, femto-SMILE, femto-cataracts and AMD.

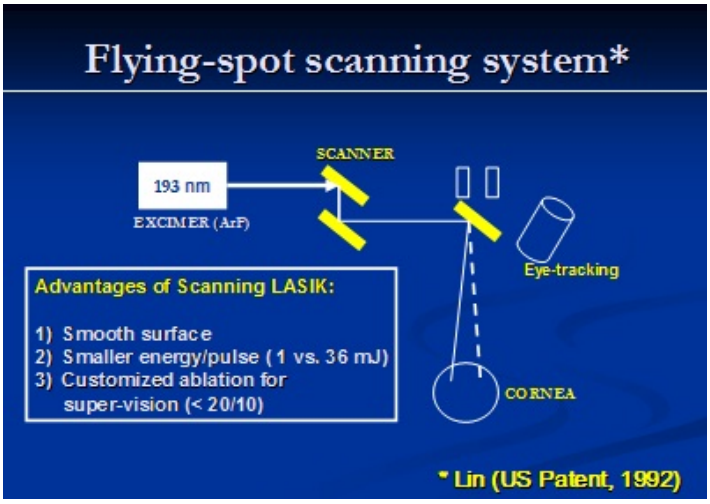

Figure 2: Flying spot scanning Lasik system using an excimer laser (at 193 nm).

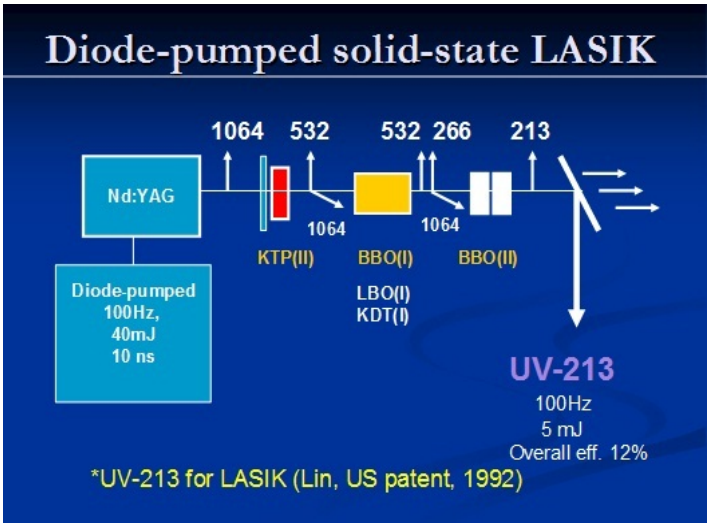

Figure 3: System for a UV solid state laser with 213 nm produced by the 5th harmonic of a diode laser pumped Nd:YAG.

The mathematics of vision corrections [4-9]

The combined technologies of scanning laser, eye tracking, topography and wavefront sensor advance the corneal reshaping (the refractive surgery) one step further from the conventional ablation of spherical surface to the customized ablation of aspherical surface.

Therefore, the theory (or mathematics) behind LASIK is also expanded from the simple paraxial formula to the high-order nonlinear formulas involving the change of the corneal asphericity and the LASIK-induced surface aberrations. Most of the existing LASIK monograms are based on spherical corneal surface. The customized nomograms require aspherical surface in order to minimize the optical aberrations.

The refractive error and AIOL [7-10]

As shown by Figure 4 for an eye model, the refractive error may be calculated by Lin's effective eye model

$$D = (1336/X - P1/Z - P2)Z2 \quad (1)$$

with Z= (1- SDc/1336). P1 and P2 are the corneal and lens power. For emmetropia (D=0), X=FZ, that is the focal point matching the retina position. The axial length L=S+X + aT, with a=0.045 and T=4.0 mm (lens thickness) and S=ACD = gT, with ADC being the anterior chamber depth.

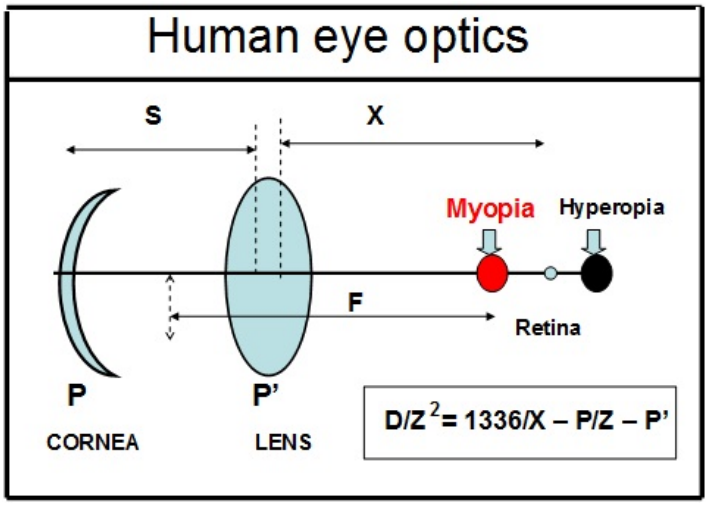

Figure 4: Human eye optics showing the image positions for myopia and hyperopia [7].

Figure 5 shows the dual-optics accommodative intraocular lens (AIOL) for the correction of presbyopia, where the red dot indicates the position of the image which could be accommodated for both near and far vision via the translation of the dual AIOL.

The total accommodation amplitude (A) may be expressed by [9]

$$A = M1(dS1) + M2(dS2) \quad (2)$$

where dS1 and dS2 represent, respectively, the amount of axial movement of the front and back optics. More detail analysis of Gaisian human optics may be found in Ref. 7 and 8.

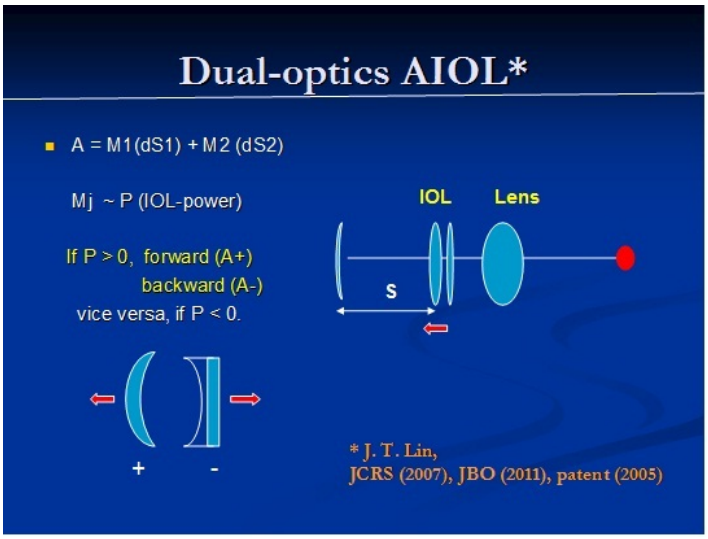

Figure 5: Dual-optics accommodative intraocular lens (AIOL). for the correction of presbyopia [10].

LASIK refractive surgery [3]

In LASIK procedure, the refractive power change is defined by the difference of the preoperative (R) and postoperative (R') front surface radius of the cornea, given by

D = 377(1/R – 1/R') (3)

where D in diopter (or 1/m) and R and R' in mm. Therefore, myopia (D<0), R'>R and hyperipia (D>0), R'<R. For examples, for a preoperative R=7.7 mm, D=(-1,-5,-10,+1, +5, +10), for R'=(8.0, 8.6, 9.7,7.4,7.0, 6.4) mm. It should be noted that in LASIK procedure the change on the corneal (front) surface represents the refractive errors of the treated subject which is normally measured by a spectacle power, Ds, (at a typical vertex distance of V=12 mm) related to D (or the contact-lens power) by D= Ds/ [1 - V Ds]. For examples, Ds=(-10, -5, +5, +10), for D=(-8.9, -4.7, +5.3, +11.4).

In a spherical corneal surface, the central ablation depth (by LASIK for myopia correction) of single-zone method is given by [3]

H0 = -(DW2/3)(1+C) (4)

with C = 0.19 (W/R)2 being the high-order term, W is the ablation zone (or diameter). Most LASIK systems use a multi-zone method, for example, in a 3-zone nomogram, H0 is revised as H (3-zone) = f H0 (single-zone), where the reduction factor f=(0.70 to 0.85) depending on the algorithms defining the power and radius of each zone. For example, comparing to a single zone with W=6.5 mm, a multizone depth will reduces to 71.6% (or f=0.716) when a smaller inner zone of 5.5 mm is used.

LASIK procedure speed

By defining T*=T/D, or the procedure time (in seconds) per diopter correction (D), one may obtain the following scaling law:

T * ~ W2/(AHPR2) (5)

where W is ablation effective zone diameter, A is the ablation rate (um/pulse), H is laser repetition rate , P is laser power (in W), and R is the laser spot size (radius). The laser fluence is defined by the laser energy/pulse per unit area F=E/(πR2). The following examples may be obtained from above equation. For a typical system parameters of W=6.0 mm, H=100 Hz, P=100 mW, E=1.0 mJ/pulse and spot size of R=1.0 mm (diameter) and ablation rate of A=0.5 microns/pulse, we define a typical T*=5.0 seconds in myopia correction. T*=(2.5, 10) seconds for H=(200, 50) Hz. Therefore for H<100 Hz, a larger spot size of R>1.2 mm would be needed for reasonable T*. For fixed (A,P,H,W), T* ~ R2, therefore T*=(20, 13.9, 3.47) seconds, for R=(0.5, 0.6, 1.2) mm. This is the major reason that a small spot system such as a diode-pumped laser system made by Custom Vis having a small energy/pulse about 1.0 mJ and spot size of 0.6 mm, requires a very high repetition rate of H>500Hz. On the other hand, for lower H<100 Hz, larger spot of >1.2 mm is needed.

Femtosecond laser surgery

One may use a femtosecond laser to ablate or remove a small portion of the lens and change its curvature (R1), where each 1% reduction may cause a 0.05 to 0.06 diopter change, based on our Gausian formula. This procedure is not as effective as that of corneal ablation (LASIK). However, ablation of the lens has no thickness limitation like a cornea. Therefore one may ablate the lens to restore a 40% change of its front surface curvature resulting 2.0 to 2.4 diopter accommodation. The current femtosecond laser has a very low average power and therefore lens ablation could take a much longer time than a corneal surface ablation in LASIK.

Scleral ablation for presbyopia treatment [5]

Scleral laser ablation and band expansion have been used to increase the space of the ciliary-body and zonus such that accomondation is improved by two components: the lens translation and the lens shaping which are given by, respectively, M7 and M3. For older and/or harder lens, the accommodation is mainly attributed by the lens translation (or S1 change), whereas lens shaping dominates the power change in young or soft lens. It was known that change of the rear surface of the lens is about one-third of the front surface during accommodation.

Optical aberration [8]

The human eye typically has a negative Q for corneal surface and positive Q for the lens surface, in which whole eye optical aberration may be partially balanced by these two opposite components, particularly in young eyes. The shape factor (p) is related to the asphericity (Q) by p=Q+1, where Q=0 (or p=1) representing a spherical surface. It was well known that the shape factor or Q increases after myopic-LASIK and decreases after hyperopic-LASIK. The amount of these changes also an increasing function of the power of corrections. For examples, Defining: Q1=pre-LASIK, Q2=post-LASIK, for a myopia -5.0 D correction, Q2=1.23(Q1+1)-1. Therefore, an initial Q1=-0.1 (prolate) will result in Q2=+0.11 (oblate); and initial Q1=-0.4 result in Q2=-0.26 (less prolate). Optical aberration may be defined by the Zernike polynomials.

It was known that the prime spherical aberration (PSA) contributed from the lens is normally negative, whereas cornea has positive contribution and has larger value than that of lens. Therefore, the PSA of the whole eye in general is positive and may be expressed

as follows

W(whole eye) = W'(cornea) + W"(lens) (6)

For typical mean value of W"=-0.026 (range -0.015 to -0.04) and W' mean of +0.032 (range of 0.02 to 0.04), one expects W(whole eye) is a positive mean value of 0.005 (range of 0.002 to 0.02) depending on the shape of the cornea and lens which are also age dependent. As reported by Smith et al. that lens has negative SA, however, it is not clear what the causes are. They proposed three sources of SA: the front, back surface asphericity and the bulk refractive index distribution in addition to the age-related factors.

Therefore, customized change (or control) of the corneal asphericity for minimal SA depends on the individual lenticular SA (W"). For higher negative W", smaller Q* (of the cornea) would be needed as shown by Eq.(25). This optimal value (Q*) for minimal whole eye SA also depends on the corneal front surface radius (R) and the contribution from its posterior surface which has a typical value about -0.6.

UV-light-initiated corneal collagen crosslinking (CXL) [11-14]

CXL systems have been commercialized for years for various corneal deceases such as corneal keratoconus, corneal keratitis, corneal ectasia, corneal ulcers, and thin corneas prior to LASIK vision corrections and other potential applications such as the scleral treatment in maligan myopia, scleromalacia and low tension glaucoma. The safety dose (E*) and the efficacy of CXL are governed by the absorption coefficients, concentration, diffusion depth of the riboflavin (RF) solution, the UV light dose, irradiation duration, the cytotoxic energy threshold of endothelial cells and the corneal thickness. Figure 2 shows a corneal model and the RF concentration profiles inside the stroma collagen. The CXL procedures could be conduced (as shown by Figure 2) either with epithelium removed (epi-off) with a 0.1% riboflavin-dextran solution or with epithelium intact (epi-on) with a 0.25% riboflavin aqueous solution. The concentration profiles show that the CXL process starts from the depletion f surface RF and takes longer time to deplete the RF inside the stroma. A safety (or maximum) dose is required to protect the endothelial cells from damage.

CXL safety and efficacy, per my analytic formulas [10] 2,3, are characterized by the collective parameters of [E, I, t, A, z, D, C,q]; where E and I are the UV light energy dose (fluence) and intensity, t is the exposure time; A and D are the absorption coefficients and diffusion depth of riboflavin (RF) in the stroma having an initial concentration C; z is the depth in the stroma (or corneal thickness in epi-off); and q is the polymerization quantum efficient. A is further defined by A=(a+b)C + Q, with a and b are the extinction coefficients of the RF and the photolysis product, and Q is the absorption constant of stroma (without RF).

Crosslink depth (Z) is defined by the depth where the RF concentration is almost depleted (to a level of <13%) given by

Z=[ln(E) + 0.44]/A (7)

with A'=[(bC+Q)(1-15.4/E)], for C=0.1%. For examples; Z=(322, 405) um, for E=(4.0, 5.0) J/cm2 and C=0.1%, D=500 um. Greater detail and the theory of CXL may be found in other published papers by Lin et al. [11-14].

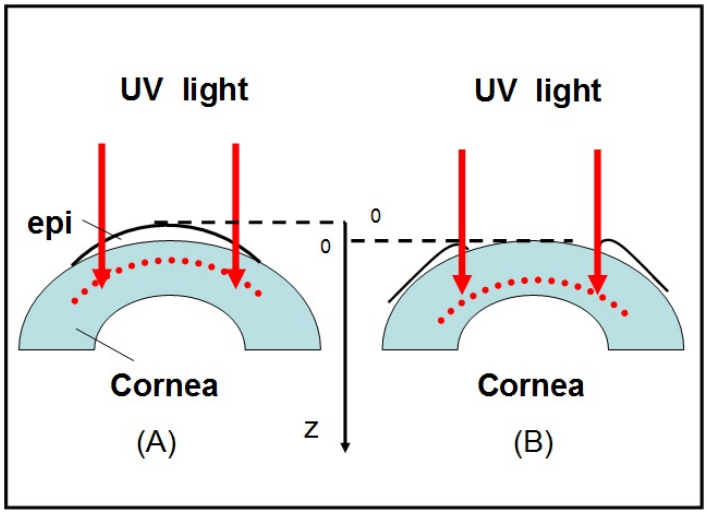

Figure 6: A corneal model system under UV light crosslinking for the epi-on (A) and epi-off (B) case (left figure) [11].

References

1. Lin JT (1992) Multiwavelength solid state laser for ophthalmic applications. Proc SPIE 1644: 266-275.
2. Lin JT (1994) Mini-excimer laser corneal reshaping using a scanning device. Proc SPIE 2131: 228-236.
3. Lin JT (1995) Critical review on refractive surgical lasers. Opt. Engineer 34: 668-675.
4. Lin JT (2005) Scanning laser technology for refractive surgery. In: Garg et al. Mastering the techniques of corneal refractive surgery. New Delhi, India, Jaypee Brothers 20-36.
5. Lin JT, Mallo O (2003) Treatment of presbyopia by infrared laser radial sclerectomy. J Refract Surg 19: 465-467.
6. Lin JT (2005) A new formula for ablation depth in three-zone laser in situ keratomileusis. J Refract Surg 21: 413-414.
7. Lin JT (2005) The generalized refractive state theory and effective eye model. Chinese J Optom & Ophthal 7: 1-6.
8. Lin JT (2016) Gaussian Optics Analysis for Human Eyes with Application for Vision Corrections. Ophthalmology Research 6: 1-5.
9. Lin JT (2006) Prediction and control of corneal asphericity after refractive surgery. J Refract Surg 22: 848-849.
10. Lin JT, Jiang M, Chang CL, Hong YL, Ren Q (2011) Analysis and applications of accommodative lenses for vision corrections. J Biomed Opt 16: 018002.
11. Lin JT, Liu HW, Cheng DC (2014) On the dynamic of UV-Light initiated corneal cross linking. J Med Biolog Eng 34: 247-250.
12. Lin JT, Cheng DC, Chang C, Yong Zhang (2015) The new protocol and dynamic safety of UV-light activated corneal collagen cross-linking. Chin J Optom Ophthalmol Vis Sci 17: 140-147.
13. Lin JT (2015) Analytic formulas on factors determining the safety and efficacy in UV- light sensitized corneal cross-linking. Invest Ophthalmol Vis Sci 56: 5740-5741.
14. Lin JT (2016) Combined analysis of safety and optimal efficacy in UV-light-activated corneal collagen crosslinking. Ophthalmology Research 6: 1-14.